CEAS-GNC-2022-047

CEAS EuroGNC 2022
"Conference on Guidance, Navigation and Control"
3-5 May 2022 @ Technische Universität Berlin, Germany

Radar-Aided Inertial Navigation with Delayed Measurements

Marc Schneider Research Associate, University of Stuttgart, Institute of Flight Mechanics and Controls, 70569 Stuttgart, Germany. marc.schneider@ifr.uni-stuttgart.de

Walter Fichter Professor, University of Stuttgart, Institute of Flight Mechanics and Controls, 70569 Stuttgart, Germany. walter.fichter@ifr.uni-stuttgart.de

ABSTRACT

A key requirement for orienting the seeker head of a guided missile towards the target is the knowledge about the missile's position and attitude. An inertial measurement unit determines the specific forces and the angular rates of the vehicle. This so-called inertial navigation, which integrates the angular rates and accelerations, is not sufficient for long-range interceptors due to initialization errors and sensor drift. Therefore, a navigation algorithm is proposed that fuses the inertial measurements with the measurements of the interceptor from the fire-control radar via a Multiplicative Extended Kalman filter. Compared to existing approaches, this navigation algorithm accounts for the delays in the transmission of the radar measurements. Monte Carlo simulations show that the proposed navigation algorithm improves the estimation accuracy of the position and attitude, and thus improves the predictions of the line-of-sight. This allows the seeker head to lock on to the target, setting the foundation for a successful interception. A sensitivity study proves the robustness of the algorithm to various sources of error.

Keywords: CEAS EuroGNC; Missile; Navigation; Radar; IMU; Sensor Fusion; Kalman Filter; Measurement Delay

Nomenclature

θ	=	elevation
ϕ	=	azimuth
$\mathbf{r}$	=	line-of-sight
$\mathbf{p}$	=	position
$\mathbf{f}$	=	state transition function
$\mathbf{q}$	=	quaternion
$\mathbf{T}$	=	rotation matrix
$\mathbf{a}$	=	specific force
$\boldsymbol{\omega}$	=	angular rate
$\mathbf{g}$	=	gravitational acceleration
$\mathbf{u}$	=	inertial measurements
$\mathbf{w}$	=	process noise
$\mathbf{x}$	=	state
$\mathbf{z}$	=	radar measurement

1 Introduction

The flight phases of a guided missile, also called an interceptor, can generally be divided into three phases: First, the launch phase where the interceptor leaves the launch platform and turns towards the target. Second, the midcourse phase, which is the longest phase, in which the interceptor aims to reach the target on an energy-optimal trajectory. In the last phase, the so-called endgame, the seeker of the interceptor is able to lock on to the target. A guidance law such as proportional navigation is used to steer the interceptor into the target. During the midcourse phase, the interceptor receives measurements of the target position and velocity from the fire control radar on the ground, enabling it to make corrections to its trajectory. A correct estimate of the line-of-sight (LOS), the line connecting the target and the interceptor, expressed in the body-fixed coordinate system, is crucial for correct target acquisition by the seeker and thus a successful interception. Since the body-fixed LOS is calculated from the position and attitude of the interceptor and the position of the target, the error of the body-fixed LOS is comprised of the errors from the target estimation and the interceptor navigation solution. The position of the target is estimated by the fire-control radar, whereas the position and attitude of the interceptor stem from the onboard navigation algorithm. Due to the small instantaneous field of view (FOV) of the seeker, the body-fixed LOS must be determined with sufficient accuracy to allow the seeker to lock on to the target. Once the distance to the target falls below the range of the seeker, it can lock on to the target, provided the estimated body-fixed LOS is approximately the same as the actual LOS. If the deviation of the estimated LOS from the actual body-fixed LOS is too large, the target is outside the small FOV of the seeker. Consequently, the interceptor cannot detect the target and must search for it by moving the seeker head. In extreme cases, the missile cannot acquire the target in time and thus cannot hit it.

The position and attitude of the interceptor are traditionally obtained by integrating the angular rates and specific forces measured by inertial sensors [1]. However, for long flight durations this can become problematic since a drift of the position and attitude occurs. In addition, initialization errors have a stronger influence on the prediction of these states when trajectories become longer. Consequently, the prediction of the body-fixed LOS is also subject to increasingly large errors. Therefore, the IMU measurements are fused with measurements of the interceptor's position and velocity by the fire-control radar. Already in 1979, [2] investigated the augmentation of IMU measurements with a shipboard radar. In-flight alignment with the help of a radar is described in [3]. [4] investigates the fusion of IMU measurements with GPS and radar measurements, albeit assuming no latency of the measurements. In real applications, radar measurements reach the interceptor with a delay. Methods to cope with delayed measurements are shown in [5] and [6]. The contribution of this work is the implementation of a navigation algorithm which fuses IMU measurements and radar measurements similar to the approach proposed by [4], but with delayed radar measurements. A multiplicative extended Kalman filter (MEKF) is developed to fuse the measurements. After describing the inertial navigation in section 2, the proposed navigation algorithm is explained in section 3. The performance of the algorithm is demonstrated in section 4 by Monte Carlo simulations and discussed in section 5. Finally, section 6 summarizes the results and provides an outlook for further work.

2 Inertial Navigation

2.1 Relative Geometry

After the launch, the interceptor receives information about the position and velocity of the target. Due to the small instantaneous FOV of the seeker, the LOS in the body-fixed system has to be determined with sufficient accuracy. Figure 1 shows the LOS. It is calculated by the position $\mathbf{p}$ of the interceptor (index M) and the target (index T).

$$\mathbf{r} = \mathbf{p}_T - \mathbf{p}_M = \begin{pmatrix} p_{T,x} \\ p_{T,y} \\ p_{T,z} \end{pmatrix} - \begin{pmatrix} p_{M,x} \\ p_{M,y} \\ p_{M,z} \end{pmatrix} \tag{1}$$

To represent the LOS in the body-fixed coordinate system, a transformation from the geodetic (index g) to the body-fixed (index b) coordinate system is needed in the form of a rotation matrix T_{bg}. It is calculated from the quaternion $\mathbf{q}_M$, which describes the attitude of the interceptor. A quaternion describes a rotation around the rotation axis $\mathbf{e} = (e_1, e_2, e_3)$ by the rotation angle α. It consists of a scalar quantity as the first entry and a vector quantity. Since four entries are used, singularities, like the so-called "gimbal lock", can be avoided.

$$\mathbf{q} = \begin{pmatrix} \cos(\alpha) \\ \mathbf{e}\sin(\alpha) \end{pmatrix} = \begin{pmatrix} \cos(\alpha) \\ e_1\sin(\alpha) \\ e_2\sin(\alpha) \\ e_3\sin(\alpha) \end{pmatrix} = \begin{pmatrix} q_1 \\ q_2 \\ q_3 \\ q_4 \end{pmatrix} \tag{2}$$

$$\mathbf{T}_{bg}(\mathbf{q}) = \begin{pmatrix} (2(q_1^2+q_2^2)-1 & 2(q_2q_3+q_1q_4) & 2(q_2q_4-q_1q_3) \\ 2(q_2q_3-q_1q_4) & 2(q_1^2+q_3^2)-1 & 2(q_3q_4+q_1q_2) \\ 2(q_2q_4+q_1q_3) & 2(q_3q_4-q_1q_2) & 2(q_1^2+q_4^2)-1)) \end{pmatrix} \tag{3}$$

It is apparent that the body-fixed LOS depends on the relative position in the geodetic system and the attitude of the interceptor, as well as the position of the target. Thus, an accurate estimation of these quantities is required.

$$\mathbf{r}_b = \mathbf{r}_b(\mathbf{r}_g, \mathbf{q}_M) \tag{4}$$

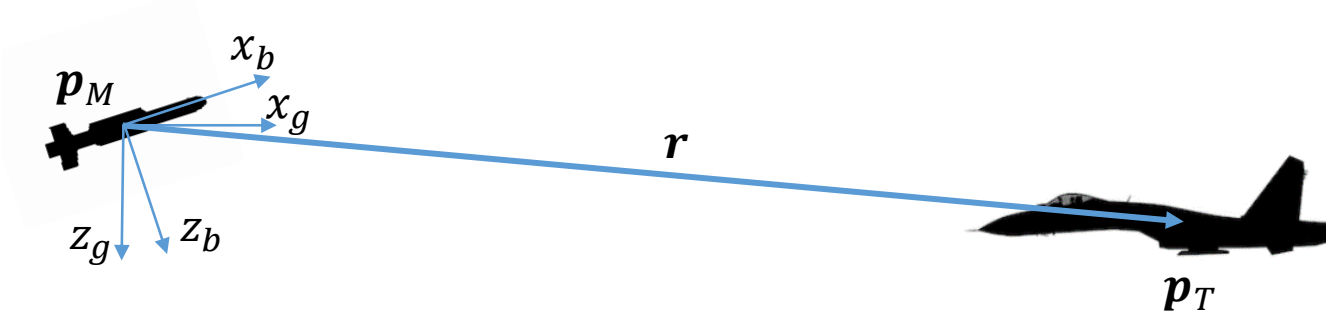

Fig. 1 Visualization of the line-of-sight.

2.2 Inertial Sensors

Classically, $\mathbf{p}_M$ and $\mathbf{q}_M$ are determined by integrating the measurements from the inertial measurements. For this purpose, the interceptor is equipped with an accelerometer to measure the specific forces $\mathbf{a}_b$ and a gyroscope to measure the angular rates ω_b in the body-fixed system with respect to the geodetic system. If these sensors are combined, they form the inertial measurement unit (IMU).

$$\mathbf{a}_b = \begin{pmatrix} a_x \\ a_y \\ a_z \end{pmatrix} = \ddot{\mathbf{p}}_M + \mathbf{g} \tag{5}$$

$$\omega_b = \begin{pmatrix} p \\ q \\ r \end{pmatrix} \tag{6}$$

Nowadays, so-called strapdown-IMUs are used, where the sensors are attached to the structure, in this case the airframe of the missile. Small semiconductor sensors, so-called MEMS ("microelectromechanical systems") enable small size and low power requirements while maintaining high accuracy. When measuring specific forces and angular rates, measurement errors occur. They can be divided into stochastic errors (which are different for each measurement) and systematic errors (which are constant over the course of a trajectory, but different for each simulation). Both of the errors follow a normal distribution with mean zero. Their properties are listed in Table 1.

	Specific force measurement	Angular rate measurement
Random Walk (PSD)	$85\ \text{micro} - \text{g}/\text{Hz}^{1/2}$	$0.125\ \text{deg}/\text{h}^{1/2}$
Standard deviation of the bias	$0.1\ \text{m}/\text{s}$	$1\ \text{deg}/\text{h}$
Standard deviation of the scale factor	$3 \cdot 10^{-4}$	$1.5 \cdot 10^{-4}$
Sampling rate	100 Hz	100 Hz

Table 1 Properties of the IMU (from [4]).

2.3 Pure Inertial Navigation

With the help of the initial conditions, numerically integrating the IMU measurements yields the position, velocity, and attitude of the missile. The following differential equation displays the change in attitude:

$$\dot{\mathbf{q}} = \frac{1}{2}\mathbf{q} \bigotimes \begin{pmatrix} 0 \\ \omega_b \end{pmatrix} \tag{7}$$

The position and velocity can be determined by integrating the acceleration:

$$\dot{\mathbf{v}} = \mathbf{T}_{gb}\mathbf{a}_b + \mathbf{g} \tag{8}$$

$$\dot{\mathbf{p}} = \mathbf{v} \tag{9}$$

Due to the measurement errors and the discretization caused by the finite sampling rate, these integrated values drift, which causes the difference between the true and the predicted body-fixed LOS to grow over time. Particularly for guided missiles with long flight durations, this drift can increase to

the point where the target may be outside the seeker's instantaneous FOV when the target moves within range of the seeker.

3 Radar-Aided Inertial Navigation

Due to the drift of the position and attitude of the interceptor as well as the dependence on initialization values, an algorithm is proposed that supplements the inertial navigation with the measurements of the interceptor's position and velocity from the fire-control radar. By fusing inertial sensor data with radar data, the prediction of the body-fixed LOS is improved, so that the target is less likely to be outside the seeker's instantaneous FOV when moving within its range.

A Kalman filter is used for this purpose. It is an iterative algorithm that generates a prediction of the new state based on its last estimate and then corrects it using a measurement to obtain an optimal estimate of the new state. In particular, it allows the estimation of system states that are not directly measurable, such as the attitude of the missile.

Due to the nonlinear state transition function and the nonlinear measurement function and their nonlinear errors, a multiplicative extended Kalman filter (MEKF) as described in [7] is used for the estimation of the states of the interceptor. An extended Kalman filter (EKF) estimates the states of the target. Compared to the measurements of inertial sensors, the radar measurements have two disadvantages: First, the sampling rate is significantly lower, and second, the measurements arrive at the missile with a delay. These effects must be taken into account in the development of the MEKF.

3.1 Radar Measurements

The fire-control radar measures the distance $\|\mathbf{p}\|$ from the fire-control radar to the tracked object, as well as the elevation θ and azimuth ϕ. The tracked object can be the target or the interceptor. Additionally, the Doppler effect can be used to determine the velocity v_{cl} of the object in the radial direction. This information represents the measurement $\mathbf{z}$, which is used to correct the prediction of the state.

$$\mathbf{z} = \begin{pmatrix} \phi \\ \theta \\ \|\mathbf{p}\| \\ v_{\mathrm{cl}} \end{pmatrix} \tag{10}$$

Tables 2, 3, and 4 depict the properties and errors of the radar measurements. Since a ground-based radar is assumed for this simulation, the misalignment of the radar is reduced by 50% compared to [4].

Variable	**Value**
Sampling rate f_R	1 Hz
Latency	1 s
First measurement after launch	5 s

Table 2 Properties of the radar measurements (partly from [4]).

Error	Standard deviation
Distance	5 m
Elevation	$3 \cdot 10^{-3}$ rad
Azimuth	$3 \cdot 10^{-3}$ rad
Closing speed	5 m/s

Table 3 Stochastic errors of the radar measurements (from [4]).

Error	Standard deviation
Misalignment of the fire-control radar station	8.5 mrad
Position of the radar station	10 m

Table 4 Systematic errors of the radar measurements (adapted from [4]).

3.2 Multiplicative Extended Kalman Filter for the Navigation of the Interceptor

The state to be estimated is comprised of the position $\mathbf{p}_M$, velocity $\mathbf{v}_M$, and attitude $\mathbf{q}_M$:

$$\mathbf{x}_M = \begin{pmatrix} \mathbf{p}_M \\ \mathbf{v}_M \\ \mathbf{q}_M \end{pmatrix} \tag{11}$$

The measurements of the IMU (denoted by the overline) consist of the true values $\mathbf{u}_M$ and the normally distributed measurement errors $\mathbf{w}_M$. They are used for the prediction step with the state transition function $\mathbf{f}_M$:

$$\mathbf{u}_M(k) = \begin{pmatrix} \mathbf{a}(k) \\ \boldsymbol{\omega}(k) \end{pmatrix} \tag{12}$$

$$\begin{pmatrix} \bar{\mathbf{a}}(k) \\ \bar{\boldsymbol{\omega}}(k) \end{pmatrix} = \begin{pmatrix} \mathbf{a}(k) \\ \boldsymbol{\omega}(k) \end{pmatrix} + \mathbf{w}_M(k) \tag{13}$$

$$\mathbf{x}_M(k+1) = \mathbf{f}_M(\mathbf{x}_M(k), \mathbf{u}_M, \mathbf{w}_M(k)) = \begin{pmatrix} \mathbf{p}_M(k+1) \\ \mathbf{v}_M(k+1) \\ \mathbf{q}_M(k+1) \end{pmatrix} = \begin{pmatrix} \mathbf{p}_M(k) = \Delta t \mathbf{v}_M(k) + \frac{1}{2}\Delta t^2 (\mathbf{T}_{gb}(k)\bar{\mathbf{a}}(k) + \mathbf{g}) \\ \mathbf{v}_M(k) + \Delta t (\mathbf{T}_{gb}(k)\bar{\mathbf{a}}(k) + \mathbf{g}) \\ \mathbf{q}_M(k) + \frac{1}{2}\Delta t \begin{pmatrix} 0 & -\bar{\boldsymbol{\omega}}(k)^\mathsf{T} \\ \bar{\boldsymbol{\omega}}(k) & -[\bar{\boldsymbol{\omega}}(k)]_\times \end{pmatrix} \end{pmatrix} \tag{14}$$

The estimation error $\mathbf{e}$ consists of only nine components, in contrast to the state, which consists of ten components.

$$\mathbf{e}_M = \begin{pmatrix} \mathbf{e}_{\mathbf{p},M} \\ \mathbf{e}_{\mathbf{v},M} \\ \mathbf{e}_{\mathbf{q},M} \end{pmatrix} \tag{15}$$

The reason for this is the representation of the error $\mathbf{e}_{\mathbf{q},M}$ in the four-dimensional quaternion by the twofold of the three-dimensional Gibbs vector $\mathbf{g}_M$. This serves as the representation of a change of the attitude compared to a reference quaternion and can be calculated as follows:

$$\mathbf{q}(k) = (4 + \mathbf{e}_{\mathbf{q},M} \cdot \mathbf{e}_{\mathbf{q},M})^{-\frac{1}{2}} \bigotimes \mathbf{q}_{\text{ref}}(k) \tag{16}$$

With the help of the radar measurements, the prediction of the state and covariance matrix can be updated. This process is described in detail in [8]. Classically, in a Kalman filter, a correction step is performed after each prediction step to correct the prediction of the state with the measurement of the fire-control radar. However, the fire-control radar with a sampling rate of 1 Hz operates with a sampling rate which is two orders of magnitude smaller than the IMU with a sampling rate of 100 Hz. Thus, to account for all acceleration and rotation rate measurements, the MEKF must predict a new state after each of these measurements. This means that there are 100 prediction steps between the correction steps. Another difficulty is that the radar measurements are received by the interceptor with a delay of one second, which corresponds to 100 IMU measurements. This known delay has to be incorporated in the MEKF design. [6] gives an overview of methods where delayed measurements are processed in the Kalman filter. Due to the large delay of 100 steps, augmenting the state vector is not viable, as the state vector would be expanded by four (the size of the measurement) times 100 (the delay) states which only makes this method suitable for small delays. The method proposed in [5] is not feasible either, since the measurement matrix is not perfectly known when the measurement is made. This method also does not allow for delays larger than the time between two measurements (i.e. in this work, the latency of one second would be the upper limit) and the delay of the measurement has to be known in advance.

Therefore, the method of recalculating the filter is implemented in this work. The measurements, state estimations, and covariance matrices need to be stored until the measurement data is available. Then the filter is restarted at the time the measurement was made. Thus, it is not the current state and the current state covariance matrix that are corrected, but those that were predicted 100 steps earlier, at the time the radar measurement was made. Figure 2 shows the MEKF process: At time step $k+100$ the radar measurement made at time step k reaches the interceptor. Thus, the state at time step k is corrected retroactively (correction). Subsequently, this corrected state is predicted again up to the current time step $k+100$ (2nd prediction). Starting from this predicted corrected state, the state is predicted for each time step using the inertial sensor measurements (1st prediction). After another 100 steps, i.e. at time step $k+200$, the state at time step $k+100$ can be corrected using the radar measurement at time step $k+100$ and can then be predicted up to time step $k+200$. By using a delayed measurement, the quality of the estimate is reduced because the received measurement is old and information is lost. This manifests itself in the accumulation of process noise.

3.3 EKF for the Estimation of the Target State

To predict the LOS in the body-fixed system, the position of the target has to be estimated. This is achieved by the following EKF. As a prediction model, a horizontal straight flight with a Gaussian velocity noise with a power spectral density of $S_{xx,T} = 10\ \text{m}^2/\text{s}$ is used:

$$\mathbf{x}_T(k+1) = \begin{pmatrix} \mathbf{p}_T(k+1) \\ \mathbf{v}_T(k+1) \end{pmatrix} = \begin{pmatrix} p_{T,x}(k+1) \\ p_{T,y}(k+1) \\ p_{T,z}(k+1) \\ v_{T,x}(k+1) \\ v_{T,y}(k+1) \\ v_{T,z}(k+1) \end{pmatrix} = \mathbf{f}_T(\mathbf{x}_T(k), \mathbf{w}_T(k)) = \begin{pmatrix} \mathbf{p}_T(k) + (\mathbf{v}_T(k) + \mathbf{w}_T(k))\Delta t \\ \mathbf{v}_T(k) + \mathbf{w}_T(k) \end{pmatrix} \tag{17}$$

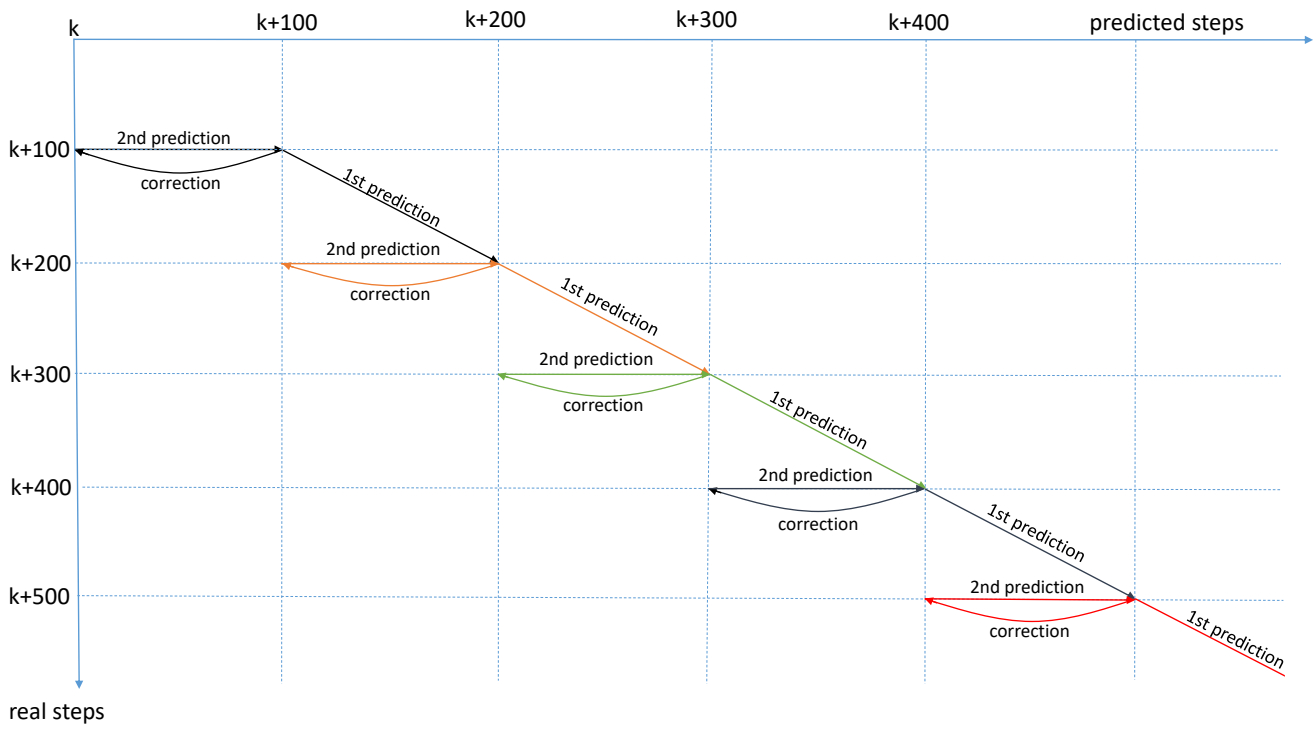

Fig. 2 Algorithm structure of the multiplicative extended Kalman filter with delayed measurements.

The predictions are corrected with radar measurements of the target, which are subject to the same systematic errors and properties as the radar measurements of the interceptor. Consequently, the filtering process is also the same with the exception of the different prediction model.

4 Simulation Results

The navigation algorithm in the form of the MEKF and the EKF for the estimation of the target states presented in the previous section were implemented in MATLAB to evaluate their performance in simulation. The assumed scenario is a target flying towards the interceptor launch position in a horizontal straight flight. The interceptor launches vertically when the target reaches its initial position and then follows a ballistic trajectory to hit the target. After about 172 seconds and 54 kilometers the interceptor hits the target. The fire-control radar, which is situated at the origin of the coordinate system, is described in section 3.1. Table 5 depicts the other parameters used in the simulation.

Since the prediction process is characterized by randomness (stochastic measurement errors, systematic measurement errors that are different in each simulation run, and random initialization errors) the entirety of multiple simulation runs must be considered. For this purpose, Monte Carlo simulations were performed. 1,000 simulation runs form one Monte Carlo simulation. The mean values and their standard deviations (as a measure of the uncertainty of the mean) of particular quantities were obtained through the simulation. They were examined in different scenarios: First, the root mean square (RMS) of the difference in direction between the true LOS in the body-fixed system and the predicted LOS in the body-fixed system using the previously outlined algorithms was evaluated. Second, since the seeker head must be oriented along the predicted LOS in the body-fixed system, the percentage of targets that are outside the seeker's instantaneous FOV when the target is in range is used as a performance metric. This criterion is decisive for the actual application of the navigation algorithm to the interceptor, as it is critical to the target acquisition, and thus the successful interception of the target.

Variable	Value
Target initial position (NED)	$(88{,}465.45, 0, -9000)^\mathsf{T}$ m^2/s
Target velocity (NED)	$(-200, 0, 0)^\mathsf{T}$ m
Target velocity spectral density	10 m^2/s
Seeker range	6,000 m
Seeker instantaneous FOV	14°
Interceptor launch position	$(50, 0, 0)^\mathsf{T}$ m
Interceptor launch mass	300 kg
Interceptor fuel mass	100 kg
Interceptor mass flow	20 kg/s
Interceptor specific impulse	250 s
Interceptor drag area	0.0014 m^2
Radar position	$(0, 0, 0)^\mathsf{T}$ m

Table 5 Simulation parameters.

4.1 Comparison between Radar-Aided Inertial Navigation and Pure Inertial Navigation

The improvement of the prediction of the body-fixed LOS by supporting the inertial navigation with radar measurement data is investigated in this subsection. For this purpose, 30 Monte Carlo simulations with 1,000 runs each are performed. Figure 3 shows the results of the simulations. Whereas the depicted mean value gives a measure of the quality of the algorithm, the plotted standard deviation gives a measure of repeatability between the mean values of the 30 Monte Carlo simulations. The root mean square error of the direction of the body-fixed LOS averaged over the 30 Monte Carlo simulations could be reduced by a factor of 4.5 compared to pure inertial navigation. The number of targets not detected (because they were outside the instantaneous field of view of the seeker) could even be reduced to about one twelfth.

Additionally, the effect of the radar measurement latency was investigated by running 30 Monte Carlo simulations with 1,000 runs each without such latency. It can be seen that the RMS value and the percentage of targets that are not detected are slightly reduced compared to the case with the measurement latency.

4.2 Sensitivity Study

To investigate the robustness of the algorithm, the influence of the parameters of the sensors on the quality of the LOS prediction was investigated. Within the scope of this sensitivity study, it is analyzed to what extent small changes of initialization errors or accuracies of the sensors affect the final angular error of the LOS. For this purpose, all parameters are kept constant except for the parameter under investigation. This parameter is then decreased or increased by 25% to investigate its influence. For each of these error factors, a Monte Carlo simulation with 1,000 runs is performed. The sensitivity study is conducted for the pure inertial navigation regarding the initialization errors and IMU errors. Figure 4 depicts the results. The error bars denote the standard deviation between the 30 Monte Carlo simulations with constant parameters (from section 4.1) to estimate the significance of the difference in the RMS values. Furthermore, the sensitivity study is conducted for the radar-aided inertial navigation, where the IMU errors and the initialization errors, as well as the errors regarding the radar, are investigated. The results are displayed in Figure 5 and Figure 6.

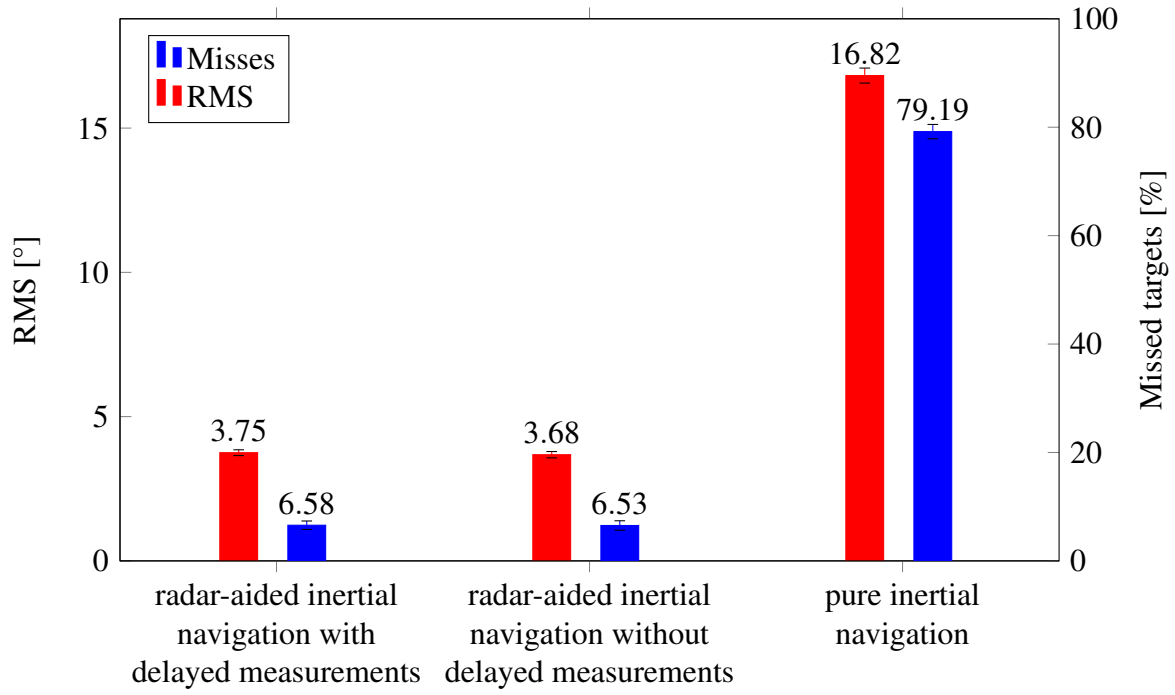

Fig. 3 Mean values and standard deviations of 30 Monte Carlo simulations with 1000 runs each.

4.3 Investigation on the Required Range of the Fire-Control Radar

In addition to the influence of initialization errors and error sources of the sensors, the dependence of the prediction on the range of the fire-control radar with respect to the interceptor is investigated. Due to the interceptor's small cross-sectional area, the range at which it can be detected by the fire-control radar might be reduced. Thus, the support of the inertial navigation with radar measurements of the interceptor may not be possible until target detection by the onboard sensor. Therefore, it is to be investigated up to which distance from the fire-control radar the navigation of the interceptor requires radar measurements. For this purpose, Monte Carlo simulations are performed with 1,000 runs per radar range, with the radar range being increased by two kilometers after each Monte Carlo simulation. The results of this investigation can be seen in Figure 7. After an initial drop in the LOS error, further increases in radar range decrease the LOS error, albeit less. Overall, it can be seen that increasing the radar range so that radar measurements of the interceptor are available until the target is hit, substantially improves the prediction of the LOS in the body-fixed system.

5 Discussion

In subsection 4.1 it could be seen, that the proposed radar-aided inertial navigation significantly outperforms the pure inertial navigation. In fact, regarding the percentage of missed targets, the pure inertial navigation would not be able to achieve a significant number of hits due to its large LOS errors. In contrast, the radar-aided inertial navigation serves as a viable navigation algorithm, achieving not only a low RMS value of the LOS deviation, but also a low number of missed targets. This allows the seeker to lock on to the target in most cases, setting the foundation for a successful interception. The reduction in the RMS value and the percentage of missed targets for the case with no measurement delay of the fire-control radar can be explained as follows: Errors in the inertial navigation result from drift and from initialization errors. Since both of them grow over time, there is simply not enough time between the correction steps to significantly alter the prediction of the position and attitude of the interceptor and the position of the target. However, this does not mean that the radar latency can be neglected in the design of the navigation algorithm. The reason for the only slightly reduced performance in the case

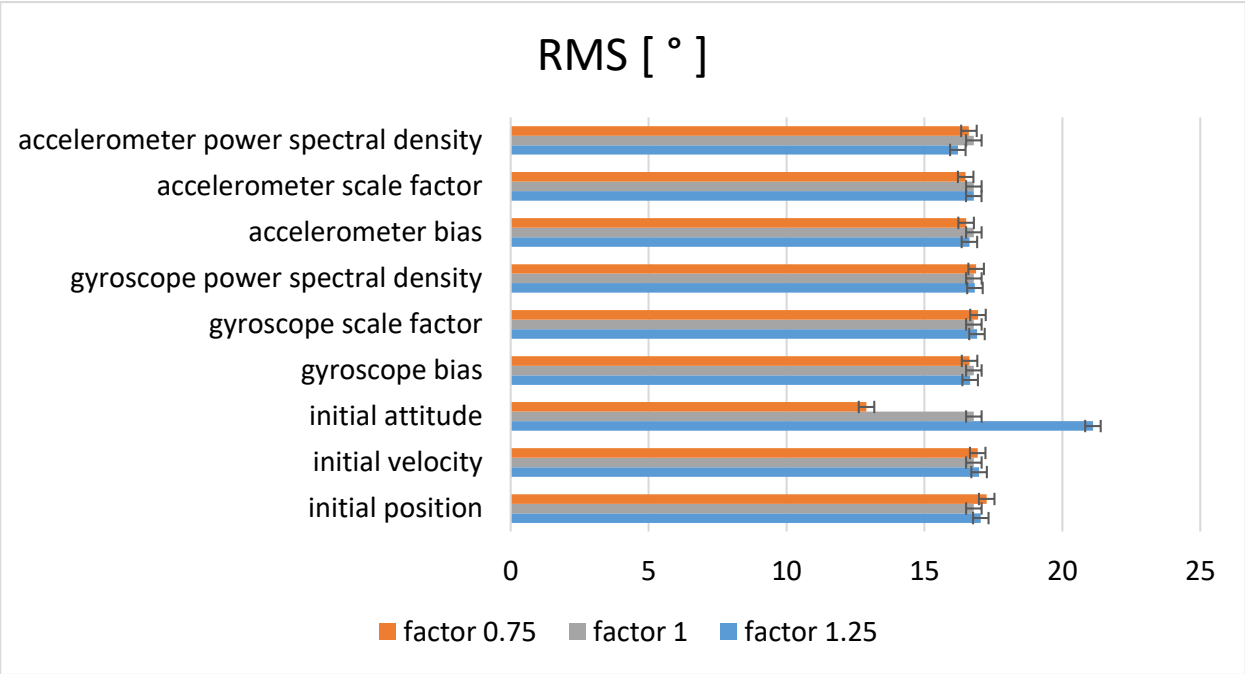

Fig. 4 Sensitivity study regarding the initialization errors and IMU errors for the pure inertial navigation.

of a radar delay is due to the aforementioned design of the MEKF. If the radar delay was not explicitly taken into consideration in the navigation algorithm and the delayed measurements were instead seen as instantaneous measurements, the estimated position of the interceptor would drift towards the delayed position, increasing the position error by hundreds of meters.

The results presented in subsection 4.2 show that the prediction accuracy of the pure inertial navigation regarding the body-fixed LOS depends strongly on a correct initialization of the attitude: Increasing the standard deviation of the initial attitude by 25% causes the RMS to increase by 26%. This was expected since a correct position prediction requires a correct initial attitude. The initial attitude error causes a position error proportional to the length of the trajectory. As the position of the interceptor plays an important role in the calculation of the body-fixed LOS, the prediction quality degrades. Other error sources of the pure inertial navigation have no significant effect on the final LOS prediction. Regarding the same investigation for the radar-aided inertial navigation, it is striking that the effect of the initial attitude error has been eliminated due to the position measurements contained in the radar measurements. Thus, initial attitude errors can be compensated, which is called in-flight alignment [9]. Figure 6 shows the influence of the error sources of the radar on the final LOS prediction: Most of the errors do not have a significant effect, with the exception of the radar misalignment. This systematic error might cancel out in the horizontal plane, since the azimuth is nearly identical for the estimation of the position of the target and the position of the interceptor. In contrast, systematic errors in the vertical plane do not cancel each other out, since the two vehicles in general only have the same elevation at the time of the hit and at a certain time after the launch of the interceptor.

Subsection 4.3 presents the results of the analysis regarding the required radar range with respect to the interceptor. Increases in radar range almost monotonically improve the prediction of the body-fixed LOS. The likely reason for this dependency on the radar measurements is that the LOS in the body-fixed system is a function of both the attitude of the interceptor and the position of the interceptor and the target. Thus, errors in the estimated positions cause errors in the direction of the estimated LOS. Without the correction through the radar measurements, the interceptor's estimated position and attitude drift, causing growing errors. Lastly, due to the short range of the seeker, a small error regarding the

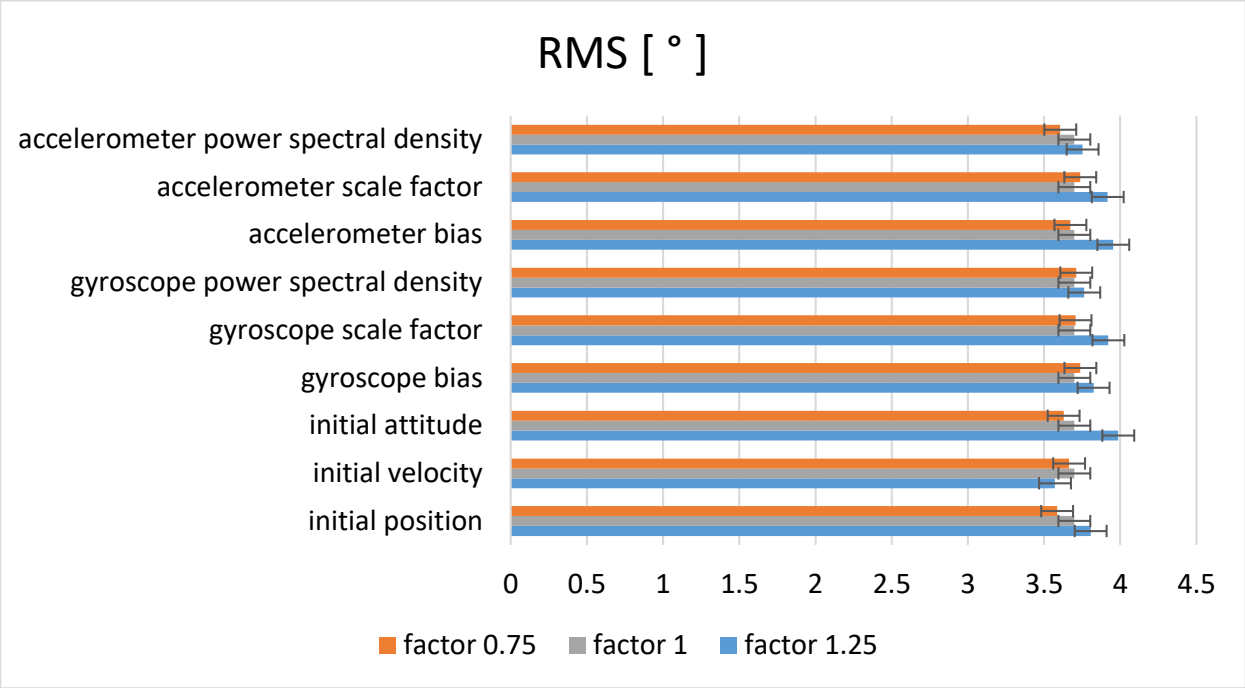

Fig. 5 Sensitivity study regarding the IMU errors and initialization errors for the radar-aided inertial navigation.

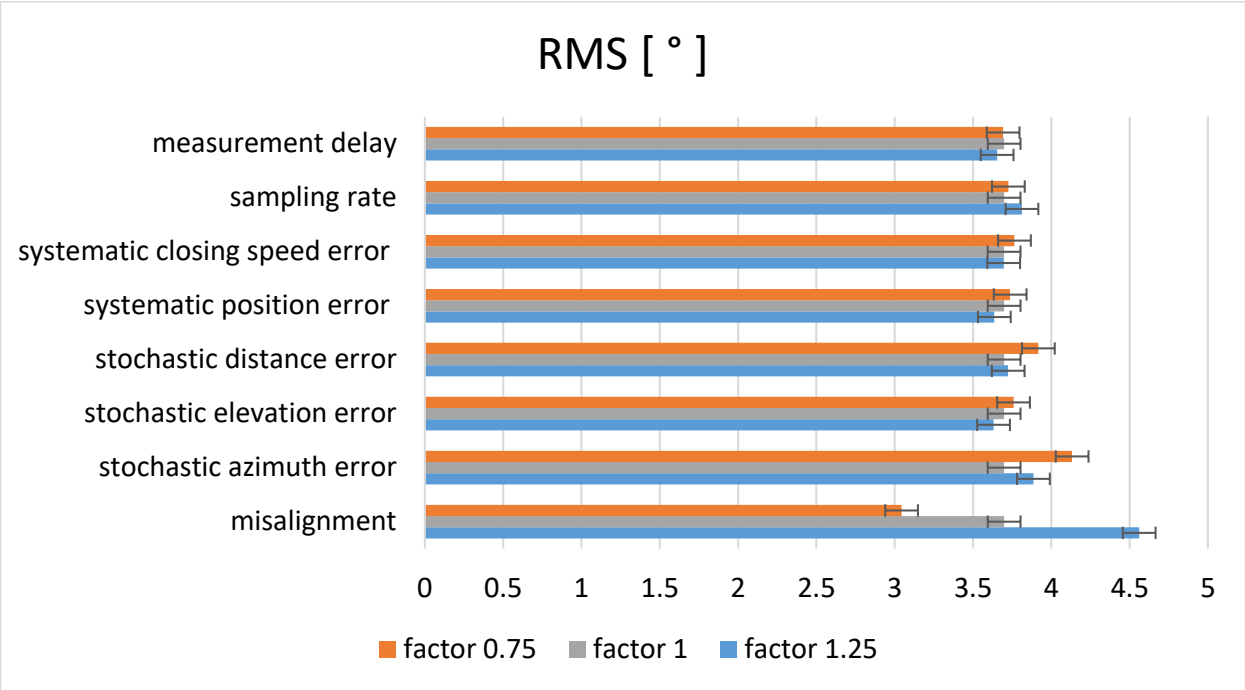

Fig. 6 Sensitivity study regarding the radar errors for the radar-aided inertial navigation.

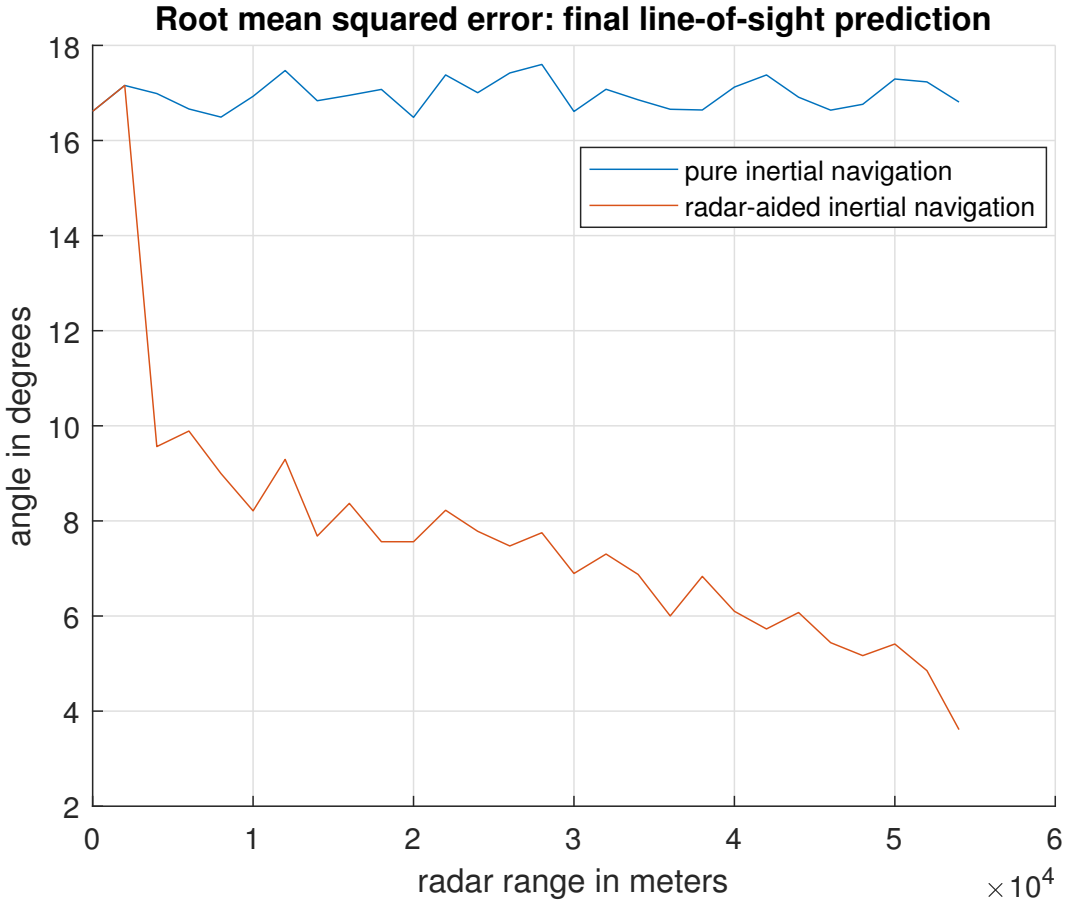

Fig. 7 LOS prediction error for different radar ranges with respect to the interceptor.

estimated position of the interceptor already causes a large deviation in the direction of the estimated LOS.

6 Conclusion and Future Work

A navigation algorithm was developed that fuses inertial measurements with delayed measurements of the fire-control radar with respect to the interceptor to create a better estimate of the interceptor's position and attitude. This allows for a more precise prediction of the body-fixed LOS to its target at the time the target comes within range of the seeker. The algorithm allows the use of intercepting missiles for long ranges, where inertial navigation, a classical approach for navigation, suffers from initialization errors and sensor drift, rendering the prediction of the body-fixed LOS almost unusable. Studies regarding the required radar range with respect to the interceptor showed that radar measurements are needed until seeker lock-on to maximize chances of a successful interception. A sensitivity study proved that the algorithm is robust against error sources which caused major prediction errors in pure inertial navigation.

Since position errors play an important role in the prediction of the LOS, the position accuracy could be improved by using multiple radar stations. Additionally, the knowledge of the state covariance matrix could be used to create an optimal search pattern in case the target is not in the seeker's instantaneous FOV.

References

[1] Oliver J Woodman. An introduction to inertial navigation. Technical report, University of Cambridge, Computer Laboratory, 2007.

[2] S BOSE. Radar updated strapdown inertial midcourse guidance performance analysis for missiles. In *Guidance and Control Conference*, page 1726, 1979.

[3] DH Titterton and JL Weston. The alignment of ship launched missile in systems. In *IEE Colloquium on Inertial Navigation Sensor Development*, pages 1–1. IET, 1990.

[4] Renato S Ornedo, Kenneth A Farnsworth, and Gurpartap S Sandhoo. Gps and radar aided inertial navigation system for missile system applications. In *IEEE 1998 Position Location and Navigation Symposium (Cat. No. 98CH36153)*, pages 614–621. IEEE, 1996.

[5] Harold L Alexander. State estimation for distributed systems with sensing delay. In *Data Structures and Target Classification*, volume 1470, pages 103–111. International Society for Optics and Photonics, 1991.

[6] Martin Bak, Thomas Dall Larsen, M Norgaard, NilsA Andersen, Niels Kjølstad Poulsen, and Ole Ravn. Location estimation using delayed measurements. In *AMC'98-Coimbra. 1998 5th International Workshop on Advanced Motion Control. Proceedings (Cat. No. 98TH8354)*, pages 180–185. IEEE, 1998.

[7] F Landis Markley. Attitude error representations for kalman filtering. *Journal of guidance, control, and dynamics*, 26(2):311–317, 2003.

[8] Ern J Lefferts, F Landis Markley, and Malcolm D Shuster. Kalman filtering for spacecraft attitude estimation. *Journal of Guidance, Control, and Dynamics*, 5(5):417–429, 1982.

[9] Scott M Bezick, Alan J Pue, and Charles M Patzelt. Inertial navigation for guided missile systems. *Johns Hopkins APL technical digest*, 28(4):331–342, 2010.